Advances in polarimetric deconvolution

Capt. Kurtis G. Engelson
Air Force Institute of Technology, Student
Dr. Stephen C. Cain
Air Force Institute of Technology, Professor

1. Abstract

One of the realities in astronomical imaging from the earth is the negative affects introduced by the atmosphere. In order to counteract the effects of the atmosphere, we propose the use of a 3 channel polarimeter and associated deconvolution algorithm. The 3 channel polarimeter features three focal plane arrays simultaneously imaging the same object through polarization analyzers set at angles of 45 and 90 degrees relative to the reference channel. The algorithm is designed to estimate the intensity of the object, its degree of polarization and a term related to its angle of polarization when performing long exposure imaging and the seeing parameter of the atmosphere is known. The results show that a degraded image of 2 point sources can be successfully reconstructed into an image resembling the actual image before the degradation occurred.

2. Introduction/Problem Statement

One major problem with imaging objects in space is the negative effects the atmosphere introduces into the imaging process. Specifically, atmospheric turbulence causes aberrations in images when viewed from the surface of earth [3:69]. Fig. 1 demonstrates the problem presented by atmospheric turbulence. This scenario shows a star that is a great distance away from the earth. The light from the star will naturally radiate in a spherical manner, but as it travels a distance of "near infinity" it can be assumed that there is a plane wave input on the lens of the telescope. The plane wave starts out untilted, but as it travels through the earth's atmosphere it is degraded.

Atmospheric turbulence causes time delays in the light as it passes through the atmosphere, but the delay is not equal amongst the entire plane wave. The curve illustrates how in this case the middle portion of the light passes through after the outsides pass through. This delay or tilt will inevitably have an effect on the image formed at the detector of camera, which is on the other side of the lens of a telescope. The lens of the telescope will cause all incoming light outside of its focal distance to converge as shown towards the bottom of Fig. 1. An ideal scenario would be that the light comes in untilted and forms an image centered on the detector, but in reality this is not the case. An input of tilted light on a lens will result in a shifted image on the corresponding detector, based on the Shift Theorem of Fourier Transforms [1:8]. After a "long" exposure time, there will not be just one shift of the point source, but an accumulation of many shifts. Fig. 1 shows a simulated example of an ideal image of two point sources, and the resulting blurry measured image at the detector. This measured image is what will be referred to from now on as measured data $d(x,y)$.

Report Documentation Page

Form Approved
OMB No. 0704-0188

1. REPORT DATE	2. REPORT TYPE	3. DATES COVERED
SEP 2010		**00-00-2010 to 00-00-2010**

4. TITLE AND SUBTITLE	5a. CONTRACT NUMBER
Advances in polarimetric deconvolution	5b. GRANT NUMBER
	5c. PROGRAM ELEMENT NUMBER
6. AUTHOR(S)	5d. PROJECT NUMBER
	5e. TASK NUMBER
	5f. WORK UNIT NUMBER
7. PERFORMING ORGANIZATION NAME(S) AND ADDRESS(ES)	8. PERFORMING ORGANIZATION REPORT NUMBER
Air Force Institute of Technology,Wright Patterson AFB,OH,45433	
9. SPONSORING/MONITORING AGENCY NAME(S) AND ADDRESS(ES)	10. SPONSOR/MONITOR'S ACRONYM(S)
	11. SPONSOR/MONITOR'S REPORT NUMBER(S)

12. DISTRIBUTION/AVAILABILITY STATEMENT

Approved for public release; distribution unlimited

13. SUPPLEMENTARY NOTES

2010 Advanced Maui Optical and Space Surveillance Technologies Conference, 14-17 Sep, Maui, HI.

14. ABSTRACT

One of the realities in astronomical imaging from the earth is the negative affects introduced by the atmosphere. In order to counteract the effects of the atmosphere, we propose the use of a 3 channel polarimeter and associated deconvolution algorithm. The 3 channel polarimeter features three focal plane arrays simultaneously imaging the same object through polarization analyzers set at angles of 45 and 90 degrees relative to the reference channel. The algorithm is designed to estimate the intensity of the object, its degree of polarization and a term related to its angle of polarization when performing long exposure imaging and the seeing parameter of the atmosphere is known. The results show that a degraded image of 2 point sources can be successfully reconstructed into an image resembling the actual image before the degradation occurred.

15. SUBJECT TERMS

16. SECURITY CLASSIFICATION OF:			17. LIMITATION OF ABSTRACT	18. NUMBER OF PAGES	19a. NAME OF RESPONSIBLE PERSON
a. REPORT	b. ABSTRACT	c. THIS PAGE			
unclassified	**unclassified**	**unclassified**	**Same as Report (SAR)**	**11**	

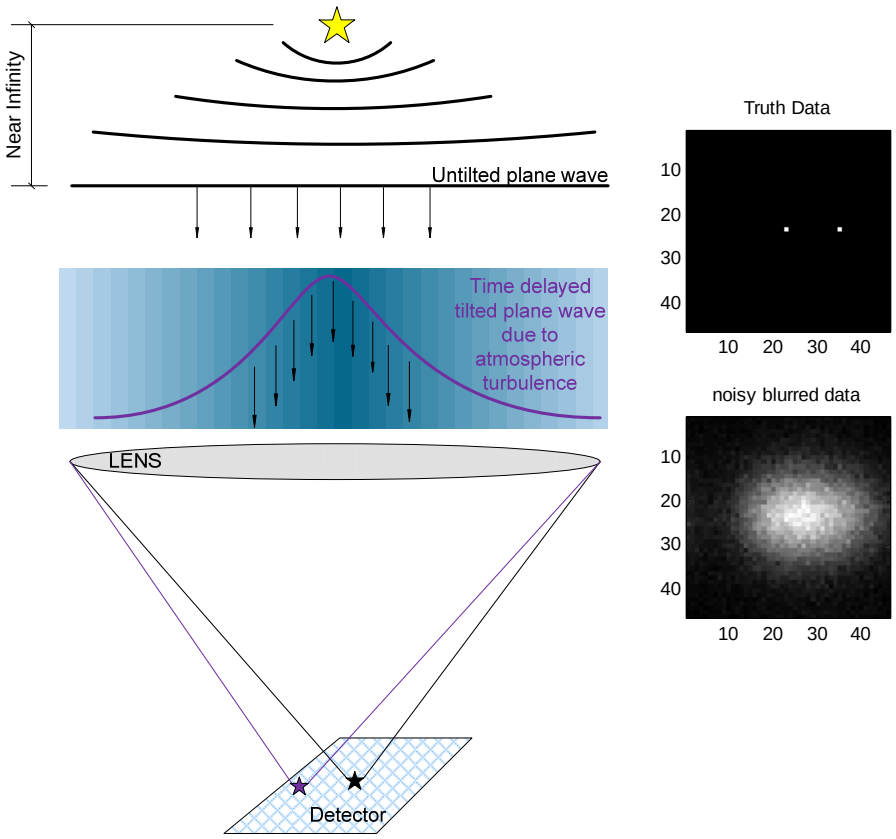

Fig. 1: Left-Atmospheric turbulence scenario. Right-Example of a 2 point source image (truth data) degraded with noise and blurring

3. Previous Work

The proposed approach to mitigating the effects of atmospheric turbulence in imaging systems is based off of a previous research effort by Captain Steven James, USAF. He researched a 2 Channel polarimetric solution. The results of his simulations showed that a 2 channel approach improved the sharpness of an image after it had been blurred by atmospheric turbulence. This paper describes an attempt to take his research one step further and investigate if adding on another channel will provide sharper images and describe the polarization state of the light [4].

4. Scenario Description

Polarimeter Setup

The proposed method for solving the three channel polarimetric deconvolution problem utilizes the Expectation-Maximization (EM) algorithm. The EM approach allows for the unpolarized image to be computed simultaneously with the degree of polarization and turbulence parameters. The three channel polarimeter is designed with each channel containing a polarization analyzer set at different angles with respect to one another. The polarization parameters are formulated so that there are no angles to estimate. Instead a single matrix is computed that is related to the squares of the sine and cosine of the angle between the analyzers and the angle of polarization in channels 1 and 2. Channels 1 and 2 are set up to be orthogonal to one another while channel 3 is set

to be at 45 degrees. This matrix removes the need to estimate an angle through a trigonometric relationship and greatly simplifies the estimation problem.

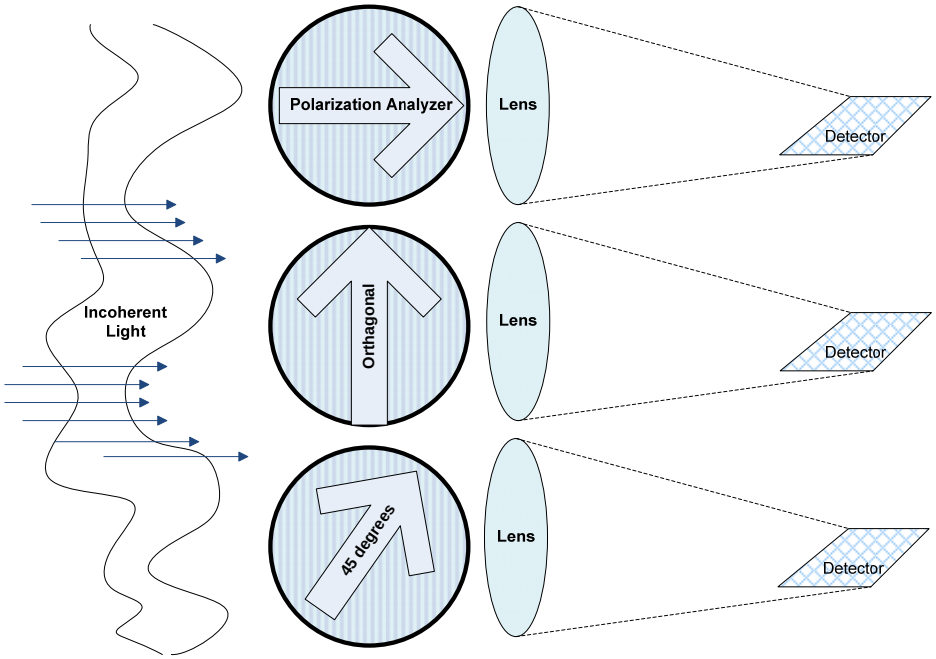

Fig. 2: Example 3 channel polarimeter set up.

Key Measurements and Assumptions

1. *Dominant source of noise is modeled with a Poisson distribution*
2. *r_0 is a known and measured value*

Equation 1 shows how the SNR is calculated for all scenarios. It also shows how one of the three variables in the denominator can be the dominant source of noise, if it is much greater than the other two. Q_n^2 represents the thermal noise, which normally comes from the camera used in observations. $E[N_b]$ is the background noise and it is the most important variable, since it is the dominating source of noise in all simulations. The main contributor of background noise is reflected sunlight, and the contribution of noise can be modeled with Poisson statistics. [3:18][5:485]

$$SNR \approx \frac{E[N_{stgxmt}]}{\sqrt{Q_n^2 + E[N_b]}} \quad (1)$$

At this point in the research phase it is also important to assume a known value for r_0 for the deconvolution to work correctly. There are ways to empirically measure r_0, therefore it is not unreasonable to assume a known value. As part of the scope of this research effort future capability to accurately measure r_0 will be added.

Optical Transfer Functions Used

The most severe degradation to the true object in Fig. 1 is caused by the long exposure optical transfer function (LEOTF). This is the OTF used to model the atmospheric turbulence for long exposure imagery ($t \gg 1/100\ \text{sec}$). The primary reason the bottom image in Fig. 2B (*d(x,y)*) looks nothing like the truth data is due to the LEOTF. The formula for the LEOTF is given by Equation 2 [5:402]. Notice that the resulting magnitude of H_{LE} is solely dependent on r_0 (Fried's Seeing Parameter [5:429]). This is only true assuming that mean wavelength of light ($\bar{\lambda}$), the focal length of the lens (f), and spatial frequency (ν) remain constant. Variables ν_u and ν_v represent the spatial frequencies, where subscripts *u* and *v* since the OTF is only relevant in the spatial frequency domain.

$$\overline{\mathcal{H}}_{LE}(\nu_u, \nu_v) = e^{-2.44\left(\frac{\bar{\lambda} f \nu}{r_0}\right)^{\frac{5}{3}}} \tag{2}$$

The least significant contribution in the blurring of the true object is due to the optics based OTF ($\mathcal{H}_0$), also known as the average OTF, given in Equation 3 [5:364]. $P(\xi, \eta)$ represents the pupil function and shows its operation in the ξ, η plane, which is the plane of the lens. The product of both OTFs gives the OTF for the system shown in Equation 4. $\overline{\mathcal{H}}_{system}$ is the OTF used for degrading all truth data.

$$\mathcal{H}_0(\nu_u, \nu_v) = \frac{\int_{-\infty}^{\infty} P(\xi, \eta) P^*\left(\xi - \bar{\lambda} f \nu_u, \eta - \bar{\lambda} f \nu_v\right) d\xi d\eta}{\int_{-\infty}^{\infty} |P(\xi, \eta)|^2 d\xi d\eta} \tag{3}$$

$$\overline{\mathcal{H}}_{system}(\nu_u, \nu_v) = \overline{\mathcal{H}}_{LE}(\nu_u, \nu_v) \mathcal{H}_0(\nu_u, \nu_v) \tag{4}$$

Deconvolution Setup/3 Channel Polarimeter Derivation Summary

The heart of this entire research effort lies in the mathematical derivation for the 3 channel polarimeter. In essence, this derivation explains the mathematics necessary to take a blurred noisy image and transform it into a sharper looking image. The six steps listed below will briefly summarize the derivation for the 3 channel polarimeter, but first it is necessary to define all of the variables in the derivation in the following table:

Table 1: Definitions of the variables for the 3 Channel Polarimeter Derivation.

Detector Plane coordinates:	x,y
Observation Plane coordinates:	z,w

Incomplete data (measured):	$d_1(x,y)$, $d_2(x,y)$, $d_3(x,y)$
Complete Data mythical:	$\hat{d}_{1UP}(x,y,z,w)$, $\hat{d}_{1P}(x,y,z,w)$, $\hat{d}_{2P}(x,y,z,w)$, $\hat{d}_{3P}(x,y,z,w)$
True image (object):	$o(z,w)$
Simulated image (intensity):	$i_1(x,y)$, $i_2(x,y)$, $i_3(x,y)$
Point Spread Function:	$h(x-z, y-w)$
Pixels, or image size:	N
Polarization parameter:	$P(z,w)$
Transmission of 3 polarizers:	$C_1(z,w)$, $C_2(z,w) = 1 - C_1$, $C_3(z,w) = 1/2 + \sqrt{C_1 C_2}$

Step 1: Obtain a Statistical Model for the Incomplete Data (Measured Data)

$$E[d_1(x,y)] = i_1(x,y) = \sum_{z=1}^{N}\sum_{w=1}^{N}\frac{1}{2}o(z,w)(1-P(z,w))h(x-z,y-w) + o(z,w)P(z,w)C_1(z,w)h(x-z,y-w) \quad ($$

Note: only half of the light is unpolarized, since the polarizer cuts half out

$$E[d_2(x,y)] = i_2(x,y) = \sum_{z=1}^{N}\sum_{w=1}^{N}\frac{1}{2}o(z,w)(1-P(z,w))h(x-z,y-w) + o(z,w)P(z,w)C_2(z,w)h(x-z,y-w) \quad ($$

$$E[d_3(x,y)] = i_3(x,y) = \sum_{z=1}^{N}\sum_{w=1}^{N}\frac{1}{2}o(z,w)(1-P(z,w))h(x-z,y-w) + o(z,w)P(z,w)C_3(z,w)h(x-z,y-w) \quad ($$

Equations 6-8 represent the mean of the 3 channels of data measured by the CCD camera. It is important to note that double sum occurs over the values z and w, which are the coordinates in the observation plane (outer-space). Notice that the intensities have coordinates in the x,y plane, also known as the detector plane (camera detector). Another key component in these equations is the PSF, h(x-z, y-w). The fact that the PSF has a relation for both coordinate systems should make it stand out. This is important, because this is the set up for a convolution to occur, and the convolution is the function that explains how objects in the observation plane will be seen in the detector plane. Lastly you'll notice the P and C's. Essentially these are just scalars on the range from (0,1).

Step 2: Invent a Set of Complete Data (Mythical)

$$d_1(x,y) = \sum_{z=1}^{N}\sum_{w=1}^{N}\tilde{d}_{1VP}(x,y,z,w) + \sum_{z=1}^{N}\sum_{w=1}^{N}\tilde{d}_{1P}(x,y,z,w) \quad (9)$$

$$d_2(x,y) = \sum_{z=1}^{N}\sum_{w=1}^{N}\tilde{d}_{2VP}(x,y,z,w) + \sum_{z=1}^{N}\sum_{w=1}^{N}\tilde{d}_{2P}(x,y,z,w) \quad (10)$$

$$d_3(x,y) = \sum_{z=1}^{N}\sum_{w=1}^{N}\tilde{d}_{3VP}(x,y,z,w) + \sum_{z=1}^{N}\sum_{w=1}^{N}\tilde{d}_{3P}(x,y,z,w) \quad (11)$$

The idea of creating complete data is to create the data we "wish" we had. We "wish" we had this data because it is supposed to be data that was never blurred by a convolution. The convolution function is the mathematical reason for the occurrence of blurring. Also note that the unpolarized complete data is the same so, $\tilde{d}_{1VP} = \tilde{d}_{2VP} = \tilde{d}_{3VP}$.

Step 3: Select a Statistical Model for the Complete Data

$$E[\tilde{d}_{1VP}(x,y,z,w)] = \frac{1}{2}o(z,w)h(x-z,y-w)(1-P(z,w)) \quad (12)$$

Where $P(z,w)=0$ in unpolarized case

$$E[\tilde{d}_{1P}(x,y,z,w)] = o(z,w)h(x\quad z,y\quad w)P(z,w)C_1(z,w) \quad (13)$$

$$E[\tilde{d}_{2P}(x,y,z,w)] - o(z,w)h(x-z,y-w)P(z,w)C_2(z,w) \quad (14)$$

$$E\left[\tilde{d}_{sP}(x,y,z,w)\right] = o(z,w)h(x-z,y-w)P(z,w)C_s(z,w) \quad (15)$$

The main goal in selecting a statistical model is ensuring statistical consistency. The complete data in this derivation was chosen to be Poisson data, because the sum of Poisson random variables is a Poisson random variable.

Step 4: Formulate the Complete Data Log-Likelihood

The complete data log-likelihood function is formulated assuming that the complete data are statistically independent. Equation 16 shows the log of the joint probability for all of the complete data.

$$L(o,h) = ln\left(P\left[\left(\tilde{d}_{1UP}, \tilde{d}_{1P}, \tilde{d}_{2P}, \tilde{d}_{3P}\right) | P^{old}(z,w), C_{1\&2\&3}^{old}(z,w), o^{old}(z,w)\right) \forall (x,y,z,w) \in Integers(1,N$$

$$= \sum_{x}^{N}\sum_{y}^{N}\sum_{z}^{N}\sum_{w}^{N}\left\{\tilde{d}_{1UP}(x,y,z,w) ln\left[{}^{1}/_{2}\, o(z,w)h(x-z,y-w)(1-P(z,w))\right] - \frac{o(z,w)h(x-z,y-w)(1}{2}\right.$$

$$+ \sum_{x}^{N}\sum_{y}^{N}\sum_{z}^{N}\sum_{w}^{N}\left\{\tilde{d}_{1P}(x,y,z,w) ln\left[o(z,w)h(x-z,y-w)P(z,w)C_1(z,w)\right] - o(z,w)h(x-z,y-w)P(z,w\right. \quad (1$$

$$+ \sum_{x}^{N}\sum_{y}^{N}\sum_{z}^{N}\sum_{w}^{N}\left\{\tilde{d}_{2P}(x,y,z,w) ln\left[o(z,w)h(x-z,y-w)P(z,w)C_2(z,w)\right] - o(z,w)h(x-z,y-w)P(z,w\right.$$

$$+ \sum_{x}^{N}\sum_{y}^{N}\sum_{z}^{N}\sum_{w}^{N}\left\{\tilde{d}_{3P}(x,y,z,w) ln\left[o(z,w)h(x-z,y-w)P(z,w)C_3(z,w)\right] - o(z,w)h(x-z,y-w)P(z,w\right.$$

$$\left. - P(z,w)^n\right.$$

Note that there has been a polarization prior added to the log-likelihood. The main reason for adding this is to constrain the values polarization to be between 0 and 1, which is "prior" known information. The PDF chosen to model this prior is a Super Gaussian, $f(P(x)) = Ae^{-2(x)^n}, P(x) \geq 0$. This PDF was chosen because it approximates a uniform PDF on (0,1) for high values of n. The log of this PDF is what is given at the very end of Equation 16. [4]

Step 5: Determine Expected Value

The conditional expected value of the complete data log likelihood must be computed in order to formulate the EM algorithm. The conditional expectations of each piece of complete data are shown below and are computed using results from Shepp and Vardi [7].

$$E\left[\tilde{d}_{1UP} | d_1\right] = \left\{\sum_{x}^{N}\sum_{y}^{N}\frac{o^{old}(z,w)(1-P(z,w))h(x-z,y-w)d_1(x,y)\,{}^{1}/_{2}}{\frac{1}{2}P^{old}(x,y)}\right\} = UNPOL \quad (17)$$

$$E[\tilde{d}_{1p}|d_1] = \left\{\sum_{x}^{N}\sum_{y}^{N}\frac{C_1^{old}o^{old}(z,w)P^{old}(z,w)h(x-z,y-w)d_1(x,y)}{i_1^{old}(x,y)}\right\} = POL1 \quad (18)$$

$$E[\tilde{d}_{2p}|d_2] = \left\{\sum_{x}^{N}\sum_{y}^{N}\frac{C_2^{old}o^{old}(z,w)h(x-z,y-w)d_2(x,y)}{i_2^{old}(x,y)}\right\} = POL2 \quad (19)$$

$$E[\tilde{d}_{3p}|d_3] = \left\{\sum_{x}^{N}\sum_{y}^{N}\frac{C_3^{old}o^{old}(z,w)P^{old}(z,w)h(x-z,y-w)d_3(x,y)}{i_3^{old}(x,y)}\right\} = POL3 \quad (20)$$

The expected value of the complete data log likelihood is added to the natural logarithm of the prior to yield the Q function: (21)

$$Q = E[L(o,h)|d_1,d_2,d_3,o^{old},P^{old},C_{1\&2\&3}^{old}] - P(z,w)^n$$

Step 6: Maximize the Expected Value

This step requires the most algebra, since the derivative of Q will be calculated and set equal to zero with respect to $o(z_0,w_0)$, and $P(z_0,w_0)$. For the sake of brevity only the results of each derivative will be shown, along with the four conditional expectations [6].

First: $\frac{\partial Q}{\partial o(z_0,w_0)}$

$$o(z_0,w_0) = \frac{\{UNPOL + POL1 + POL2 + POL3\}}{1/2\,(1-P) + PC_1 + PC_2 + PC_3} = \frac{\{UNPOL + POL1 + POL2 + POL3\}}{1/2 + P(1/2 + C_3)} \quad (22)$$

$$Where\ C_3 = \frac{POL3}{oP}\ ;\ Therefore\ o(z_0,w_0) = \frac{UNPOL + POL1 + POL2}{1/2 + P/2} \quad (23)$$

Equation 23 is referred to as the update equation for the object $o(z,w)$.

Second: $\frac{\partial Q1}{\partial P(z_0,w_0)}$

$$P^0[UNPOL + POL1 + POL2] + P^1[-2UNPOL - POL1 - POL2] + P^2[-UNPOL] - nP^n + nP^{n+} \quad (24)$$

The most important operation of the deconvolution is the estimation of $P(z,w)$. This is accomplished by solving for the roots in Equation 24. Once $P(z,w)$ has been estimated the object and C's can be estimated.

5. Results and Analysis

Preparatory Explanation of Figures:

The simulated polarimeter results are shown in Fig. 3 & 4 below. Both figures are composed of 3 images. The left image is the truth data. It represents two point sources with pixel spacing equal to 9 pixels. The two other images in each figure show the results of the deconvolution for 2 and 3 channel algorithms. The mean squared error (MSE) is displayed at the end of each figure caption. In both cases shown the 2 channel results have nearly double the MSE, compared to the 3 channel.

The figure caption also defines some other very important simulation parameters. First is the lens size in centimeters. Second is the r_0 value in centimeters. The third value requires a little explanation, since it differs from middle image to right image. To ensure consistency in comparisons the signal strengths must be relatively equal. This means that if the truth data's two point sources are represented by 200,000 photoelectrons in each white pixel in the 2 channel polarimeter, the 3 channel must have 2/3 the amount of photoelectrons, because it splits the light signal into three channels. The fourth value is the point source pixel spacing. Fifth is the number of iterations used in the deconvolution. The sixth number is the angle of polarization in the observation plane. This angle directly impacts the values of transmission shown at the bottom of Table 1. Lastly, the numbers along the x-axis and y-axis show the size of the image. Simulations for the 120 cm lens used an image size of 32x32 pixels. Simulations for the 160 cm lens used 46x46 pixel images.

160 cm Lens Results:

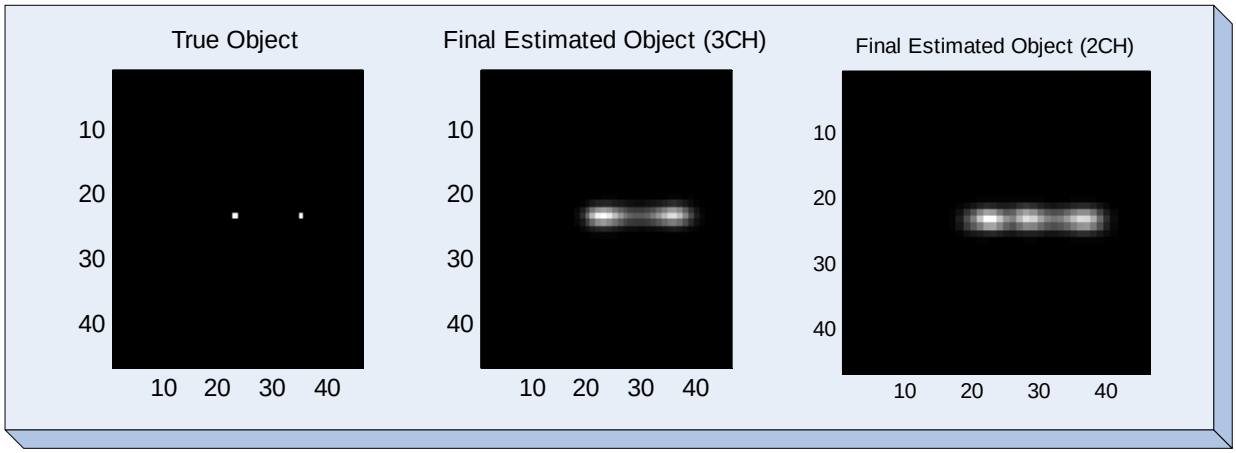

Fig. 3: Results for: Lens = 160 cm; r_0 = 15 cm; Signal Strength = 134k/200k photoelectrons; Point Source Spacing = 12 pixels; Iterations = 6000; Angle of Polarization = 300 degrees. Mean Squared Error: $3.46E^{10}$ (3CH), $8.826E^{10}$ (2CH)

120 cm Lens Results

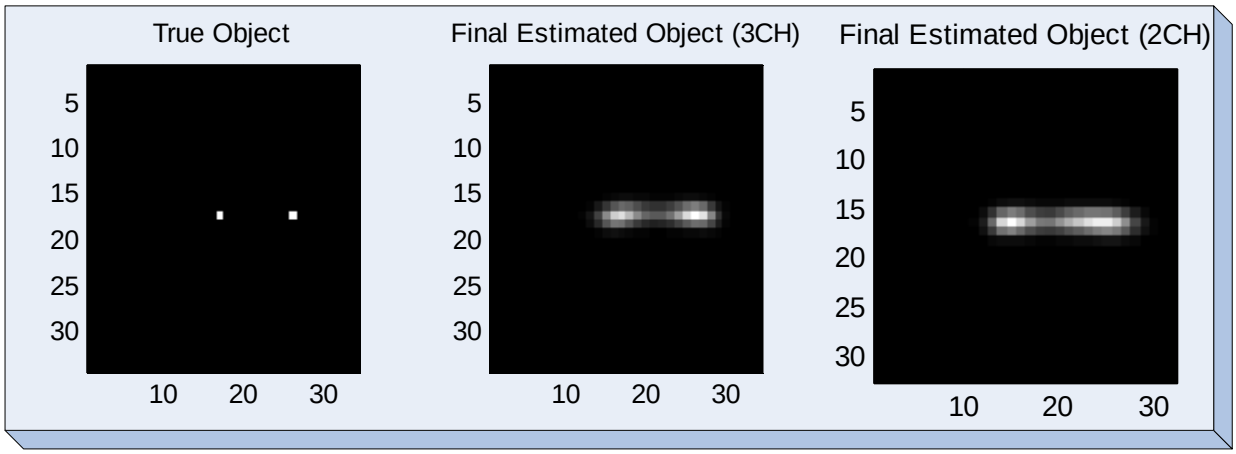

Fig. 4: Results for: Lens = 120 cm; r_0 = 15 cm; Signal Strength = 134k/200k photoelectrons; Point Source Spacing = 12 pixels; Iterations = 6000; Angle of Polarization = 123degrees. Mean Squared Error: $3.48E^{10}$ (3CH), $7.71E^{10}$ (2CH)

6. Limitations

There is one key ratio that determines how blurred an image will be after it passes through the atmosphere. This is the ratio of lens diameter to r_0 (D/r_0). A larger ratio contributes to more blurring in an image. A goal in this research is to use actual lens sizes of scopes at the observatory on top of Haleakala.

Conclusion

The degradation effects due to atmospheric turbulence can be devastating in imagery analysis. Polarization diversity is a tool that can be used to overcome the effects of the atmosphere on astronomical imagery. The 3 channel deconvolution algorithm is shown in the simulations presented here to surpass the 2 channel algorithm in overall imaging performance. This paper only discusses results based off of a dual point source image, but the 3 channel polarimeter has the potential to work for different types of astronomical imagery. There is still much work to be done in this research effort. Some future tasks include, but are not limited to: experimenting with other imagery besides two point source imagery, adding blind deconvolution capability to the 3 CH algorithms, developing stopping criteria, and compensating for thermal-camera noise as part of the solution.

REFERENCES

[1] J.W. Goodman, *Intro to Fourier Optics 3rd Ed.*, Roberts & Company, Englewood, CO, 2005.

[2] M.A. Skinner, F. Anast, J. Mooney, D. Kono, "IAO new Adaptive Optics Visible Imaging and Photometric System for AEOS," presented at the AMOS Conf., Maui, HI, Sept 2008

[3] R.D. Richmond, S.C. Cain, *Direct Detection LADAR Systems*, SPIE, Bellingham, WA, 12 March 2010

[4] S.P. James, "Beyond Diffraction Limited Seeing Through Polarization Diversity," presented at the AMOS Conf., Maui, HI, Sept 2008

[5] J.W. Goodman, *Statistical Optics 1st Ed.*, Wiley-Interscience Pubs, New York, NY, 2000

[6] A.P. Dempster, N. M. Laird, and D. B. Rubin, "Maximum likelihood from incomplete data via the EM algorithm," *J. R. Stat. Soc. B*, 39, 1-37 (1977).

[7] L. A. Shepp andY.Vardi, “Maximum likelihood reconstruction for emission tomography,” *IEEE Trans. Med. Imag.*, vol. MI-1, pp. 113–122, Oct. 1982.